CrossMark

ORIGINAL PAPER

Mechanical and rheological properties of silica-reinforced polypropylene/m-EPR blends

Anđela Pustak[1] · Matjaž Denac[2] · Andrijana Sever Škapin[3] · Iztok Švab[4] ·
Vojko Musil[2] · Ivan Šmit[1]

Abstract Rheological and mechanical properties (tensile and impact properties) as well as the mechanical profiles of ternary isotactic polypropylene/silica/elastomer (iPP/SiO$_2$/m-EPR metallocene catalyzed ethylene-propylene rubber) composites were investigated and discussed. The effects of two metallocene ethylene-propylene-based elastomers (m-EPR) differing in molecular weight/viscosity and their content on iPP/silica composites with different silica types differing in size (nano- vs. micro-) and surface properties (untreated vs. treated) were investigated. The two m-EPR elastomers were added to iPP/SiO$_2$ 96/4 composites as possible impact modifier and compatibilizer at the same time in 5, 10, 15, and 20 vol% per hundred volume parts of composites. The effects of different silica fillers and two m-EPR rubbers were discussed within the context of structure-morphology-mechanical property relationships of these iPP/SiO$_2$/m-EPR composites. Tensile and impact strength properties were mainly influenced by combined competetive effects of stiff filler and tough m-EPR elastomer so sinergistic effect was also observed. The ductility of these composites was affected additionally by spherulite size of the iPP matrix due to the difference in nucleation abilities of silica fillers enabled by prevailing separated morphology observed in iPP/SiO$_2$/m-EPR composites.

Keywords Polypropylene composites · Mechanical properties · Structure-property relationships

Introduction

Isotactic polypropylene (iPP) is one of the most widely used commodity plastomers for composites owing to its outstanding properties and versatile applications, but the most important disadvantage is very low impact resistance at the room temperature [1].

Polypropylene matrix composites with different fillers have achieved outstanding progress as advanced material. Functionalization of the filler surfaces as well as the introduction of compatibilizers and impact modifiers in such designed materials has enabled a remarkable progress in investigation of such polymer-matrix composites [1–5].

For plastic engineering isotactic polypropylene is very often modified with silica SiO$_2$ that has been used as a filler for

✉ Anđela Pustak
   apustak@irb.hr

   Matjaž Denac
   matjaz.denac@uni-mb.si

   Andrijana Sever Škapin
   andrijana.sever@zag.si

   Iztok Švab
   Iztok.Svab@isokon.si

   Vojko Musil
   vojko.musil@triera.net

   Ivan Šmit
   ismit@irb.hr

[1] Division of Materials Chemistry, Ruđer Bošković Institute, Bijenička 54, 10002 Zagreb, Croatia

[2] FEB Maribor, Institute of Technology, University of Maribor, Razlagova 14, 2000 Maribor, Slovenia

[3] Department of Materials, Laboratory for Polymers, Slovenian National Building and Civil Engineering Institute, Dimičeva 12, 1000 Ljubljana, Slovenia

[4] ISOKON, Production and Processing of Thermoplastic Ltd, Mestni trg 5a, 3210 Slovenske Konjice, Slovenia

the past two decades. The silica filler used as reinforcing agent usually affects ultimative mechanical properties and such studies have been performed mainly concerning silica nanofillers [6–12]. Mechanical testing of iPP/silica composites showed the improvements of some mechanical properties at low silica content (up to 10 % of silica filler) due to reduced agglomeration of silica nanoparticles by the silica particle surface treatment [6–13]. In order to balance the toughness and stiffness and to improve the interfacial stress transfer at the same time the compatibilizer and/or rubber toughening agents should be added to polymer composites. Compatibilization of binary and ternary iPP composites modified with fillers and different types of elastomers was widely investigated [14–25]. Introduction of polymers acting like compatibilizer and/or impact modifier in iPP/silica composites was explored in few papers with different types of elastomers added [14–25].

As one type of the rubber toughening agents (added up to 30 %) and compatibilizer (added up to 10 %) styrenic block copolymers (SBC) were introduced into polypropylene and investigated [14–19].

Wang et al. established the stiffness-toughness balance of the iPP/silica/SBR (styrene-butadiene rubber elastomer) through the synergistic effect of silica filler and (SBR) elastomer [14]. Mae et al. have investigated the iPP/SiO$_2$ composites modified with poly(styrene-b-ethylene-co-butylene-b-styrene) (SEBS) and have found that some mechanical properties strongly depended on selectivity of SiO$_2$ nanoparticles [15].

Midany and Ibrahim used SEBS and maleated SEBS (SEBS-g-MA) as compatibilizers (amounts of 5 and 10 %) and have proved good compatibilization of the iPP/SiO$_2$ interface with added elastomer [16].

Similar system iPP/SiO$_2$/SEBS but with the another added component, PP-g-MA (maleated polypropylene), acting as compatibilizer have been investigated by Panaitescu et al. and confirmed relatively good compatibility of the iPP/SEBS interface resulting in improvement of mechanical and dielectrical properties of this system [17]. Study of the iPP/silica composites modified by SEBS(−g-MA) by Pustak et al. revealed that the mechanical properties were affected mostly by combined competitive effects of stiff filler and tough elastomer [18, 19].

Bikiaris et al. [20] and Buaziz et al. [21] investigated maleated polypropylene (PP-g-MA) as a compatibilizer to binary iPP/SiO$_2$ composites and improvement of mechanical properties was achieved due to better adhesion between iPP matrix and silica particles.

The reactive compatibilization with toughening in hybrid composite system of polypropylene with silica and by elastomeric polyurethane component (PU) suggested by Chen at al. improved ductility and impact strength [22].

Another type of elastomers for providing the balance between toughness and stiffness in composites with polypropylene matrix are the elastomers based on ethylene or polypropylene coplymers, like ethylene–propylene rubber (EPR) and ethylene–propylene–diene monomer rubber (EPDM) [23–25]. Uotila et al. have studied iPP/elastomer/SiO$_2$ composites and used impact-modified block polypropylene (EPR) from Borealis as compatibilizer and observed that the selectivity of silica particles for iPP and EPR phases depended on type of applied compatibilizer [23]. Martin et al. have presented simplified PP/EPDM blend systems (double role of EPDM – as compatibilizer and impact modifier - could be supposed) with silica particles and found that relaxation and strain recovery behaviour has been greatly improved [24]. In the similar system Bazgir et al. have shown that silica particles tended to remain encapsulated by the EPDM rubber when it is mixed with EPDM before the adding of iPP and improved mechanical properties by changing the EPDM/iPP viscosity ratio in dynamically crosslinked EPDM/iPP 60/40 blend filled by silica [25]. Recent investigation of EPDM/SiO$_2$ composites by Mokhotku et al. has proved better dispersion and smaller extent of silica particles agglomeration with presence of coupling agent and also improved thermal stability and Young's modulus properties of this composites [26].

Thereby, we have applied metallocene ethylene-propylene rubber copolymers (m-EPR) with propylene being the major component (> 80 wt%). Two specialty co/terpolymers of propylene balanced with ethylene and other α-olefins with different viscosity (e.g. molecular mass) and compatible with various polyolefins were chosen under trade name Vistamaxx™ signed as m-EPR1 and m-EPR2 [27, 28]. The use of elastomeric m-EPR1 and m-EPR2 copolymers as impact modifiers/ compatibilizers (0–20 vol% per hundred volume parts of composites) at the same time simplifies the studied system to ternary iPP/SiO$_2$/m-EPR composite. On the other side, using four silica fillers differing in size (nano- vs. micro-) and the surface properties (hydrophilic vs. hydrophobic, e.g. polar vs. non-polar) enabled the comparison of different effects of filler with constant iPP/silica 96/4 content.

Accordingly, the effects of different silica fillers (added in constant content of iPP/silica 96/4) and varied contents of two m-EPR elastomers were discussed within the context of mechanical properties-morphology relationships.

Experimental

Materials

Isotactic polypropylene (trade name Novolen) used as polymer matrix was supplied by Basell, Netherlands. Sillica was used as filler: two proprietary microsilica fillers (hydrophilic Sipernat 120 and hydrophobic Sipernat D17) and two proprietary nanosilica fillers (hydrophilic Aerosil 200 and hydrophobic Aerosil R7200). All silica fillers were kindly supplied by Evonic Industries (Degussa), Essen, Germany. Two metallocene propylene-ethylene copolymers with different

viscosity are used from Exxon Mobile [27, 28]. The properties of used polymers and fillers are listed in Table 1.

Sample preparation

Ternary iPP/SiO$_2$/m-EPR composites were prepared in an oil-heated Brabender kneading chamber. The iPP/SiO$_2$ ratio was kept constant at 96/4 vol% and 5, 10, 15, and 20 vol% of m-EPR elastomer was added per hundred volume parts of iPP/SiO$_2$ 96/4 composite (phr) (e.g. added 20 vol% of elastomer corresponds to 16.7 vol% of m-EPR in total mass). Relatively wide content range 0–20 vol% of m-EPR elastomers was used in order to research its efficiency as impact modifier - not only as compatibilizer. The iPP/SiO$_2$ of 96/4 was chosen as optimal on the basis of our previous investigation of binary iPP/SiO$_2$ composites that had the best results in tensile testing and the largest observed spherulites [6, 12].

The components were put into an oil-heated Brabender kneading chamber preheated up to 200 °C with a rotor speed of 50 min^{-1} and then kneaded for 7 min. After homogenization, the melt was rapidly transferred to a preheated laboratory press and compression molded into 1- and 4-mm thick plates. The pressing temperature was 220 °C, pressure 100 bar and the pressing time of 14 min for 1-mm and 11.5 min for 4-mm thick plates.

Testing methods

Optical microscopy (OM)

A Leica light microscope (Model DMLS) coupled with a digital camera was used for morphology observation of thin crossed microtomed sections (taken from 1-mm thick plates) under crossed polarizers (POM) or phase contrast (PC). Maximal anisotropic diameter of spherulites ($d_{i,max}$) was measured on five or six polarization micrographs of each sample with Motic Images Software and average spherulite diameter (d_{sph}) was calculated according to equation (1):

$$d_{sph} = \frac{\sum N_i d_{imax}}{\sum N_i} \tag{1}$$

where N_i is the number of measured spherulites with the average diameter d_i.

Scanning electron microscopy (SEM)

A SIRION 400 NC scanning electron microscope (SEM) was used for morphology study of the ternary composites. Samples were cryofractured and gold plated before being examined with a microscope at an acceleration voltage up to 10 kV at various magnifications. All SEM micrographs are secondary electron images.

Steady state torque (τ_M)

The torque value (τ_M) was determined from the diagram of kneading in the Brabender kneading chamber. The average τ_M value was calculated on the basis of 5 measurements carried out for each sample with the same filling volume.

Tensile tests

Tensile properties (Young's modulus, tensile strength at break, elongation at break) were measured according to ISO 527 standard using Zwick 147,670 Z100/SN5A apparatus at 23 °C and strain rate of 2 mm/min. For each sample, 5 measurements were carried out.

Notched impact strength

Notched impact strength was measured by Zwick apparatus at 25 °C according to Charpy test (DIN 53453). For each sample, 12 measurements were carried out.

Results and discussion

Steady state torque of the iPP composites

The mixing torque values (τ_M) provide information how elastomeric m-EPR modifier and silica filler affect processabillity of the iPP/silica/m-EPR composites. The torque value can be considered a measure of the viscosity under the same mixing conditions, including the same filling volume. The torque τ_M increases by adding components in batch mixer and decreases after the polypropylene melting and reaches constant value around sixth minute of mixing (τ_M values in Fig. 1a,b are measured at 7th min) due to homogenization and equalized viscosity of composites [29]. While τ_M values reasonable increased with incorporation of silica fillers [12], τ_M values was negligible affected by adding of m-EPR1 elastomer (Fig. 1a), and even slightly decreased with addition of m-EPR2 elastomer (the decrease is evident in all samples at 5 vol% of added m-EPR2 in Fig. 1b). Stronger decrease of τ_M values for composites with m-EPR2 than with m-EPR1 due to lower viscosity of m-EPR2 than m-EPR1 copolymer has been observed (see MFI values in Table 1). Rheological behavior of molten composites with S-120, A-200 and S-D17 fillers is similar to behavior of composites modified with SEBS and SEBS-g-MA elastomers [18, 19]; τ_M values of composites with these three fillers are higher than for composite with treated A-R7200 nanosilica filler. Higher viscosities of molten composites with treated micro filler particles S -D17 than with treated nanoparticles A-R7200 are in an according to findings of Das et al. [30]. Namely, larger effective radii of the microparticles (as well as the agglomerates) lead to higher stress during mixing what

Table 1   The properties of used materials

Polymer	Commercial name	Density(gcm^{-3})	MFI (g10^{-1}min^{-1})	M$_n$ (gmol^{-1})	M$_w$/M$_n$	M$_w$/M$_n$
iPP	Moplen HP501L	0.90	6.0[a]	120.000[c]	5.40	
m-EPR1	Vistamaxx-VM-1100	0.863	4.5[b]	92.900[c]	3.40	
m-EPR2	Vistamaxx-VM-1120	0.863	20[b]	48.100[c]	2.66	
Filler	**Commercial name**	**Tapped density (g dm^{-3})**	**Surface modification**	**Specific surface area (m^2 g^{-1})**	**Particle size, d_{50}**	
S-120	Sipernat 120	185	none	125	14.5 μm	
S-D17	Sipernat D17	150	2 % of chem. Bounded carbon	100	10 μm	
A-200	Aerosil 200	50	none	200	12 nm	
A-R7200	Aerosil R-7200	~ 230	methacryl-silane	150	12 nm	

[a] according to ISO 1133 (230 °C/2,16 kg)

[b] according to ISO 1133 (200 °C/5 kg)

[c] measured with exclusion chromatography with PS standard

results in higher τ_M values for composite with modified S-D17 microsilica than with modified nanosilica A-R7200. Additionally, silica particles with methacrylsilanized surface with amphiphilic character (A-R7200 with polar carbonyl groups) repeal each other and lead to diminishing degree of agglomeration decreasing thus the torque value.

Moreover, composites with uncoated/untreated silica fillers with hydrophilic surfaces (S-120 and A-200) exhibit the highest τ_M values more likely to binary iPP/silica composites with these fillers [12]. Such behavior of these composites somewhat differs from composites with SEBS [18] that exhibited prevailing core-shell morphology with encapsulated silica particles and agglomerates. It indicates that fillers, hydrophilic silicas (S-120, A-200) and treated silicas (S-D17, A-R7200) in presented iPP/SiO$_2$/m-EPR composites contribute to frictional forces (i.e. τ_M values) differently due to prevailing separated morphology [31].

Somewhat higher τ_M values for composite with hydrophilic A-200 nanosilica than with hydrophilic S-120 microsilica could not be explained by the difference in interfacial areas or particles size [30] like in composites with treated (S-D17, A-R7200)

particles with opposite rheological behavior. Confirmed higher agglomeration degree of the hydrophilic than the hydrophobic silicas in binary iPP/SiO2 composites [6] could more significant affect torque at the contents higher than 4 vol% silicas [12]. The analysis of SEM micrographs of these composites at higher magnification (with S-120, A-200) exhibit the tendency of hydrophilic nanoparticles to form filler network (Figs. 2,3) due to effect of end –OH group on the surface. This fact suites well with literature finding that silica filled compounds exhibit strong Payne-effect as a consequence of the strong interparticle forces between the silica particles [32, 33].

Group of authors [34–36] have observed the formation of the filler-network structure in SEM micrographs in investigation of solid-like rheological behavior of some ternary PP/EPDM/SiO$_2$ composites prepared by two-step processing method. They supposed that hydrophilic surface of SiO$_2$ particles was necessary for the formation of filler-filler network in ternary PP/EPDM/SiO$_2$ system facilitated by increased elastomer content [34–36]. Tendency of filler network formation could be observed in SEM micrographs of composites with hydrophilic A-200
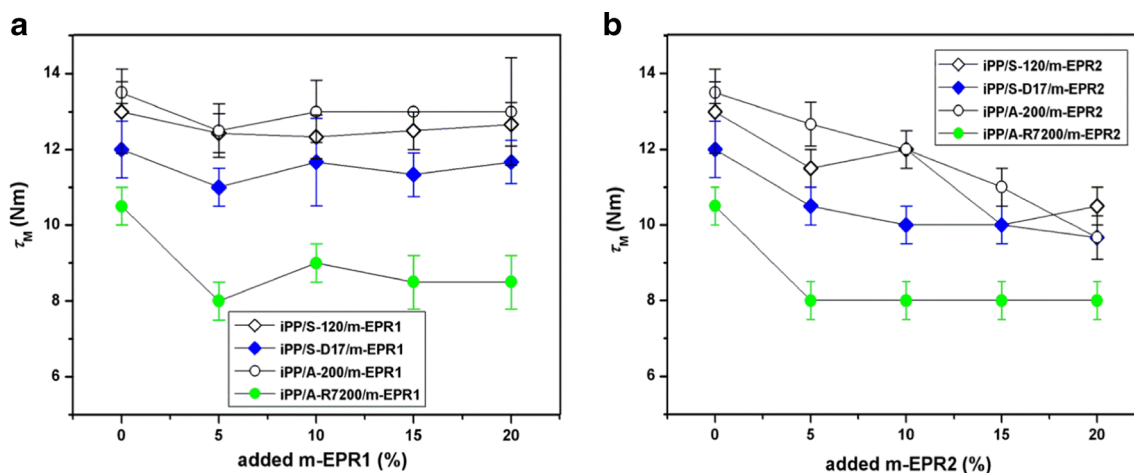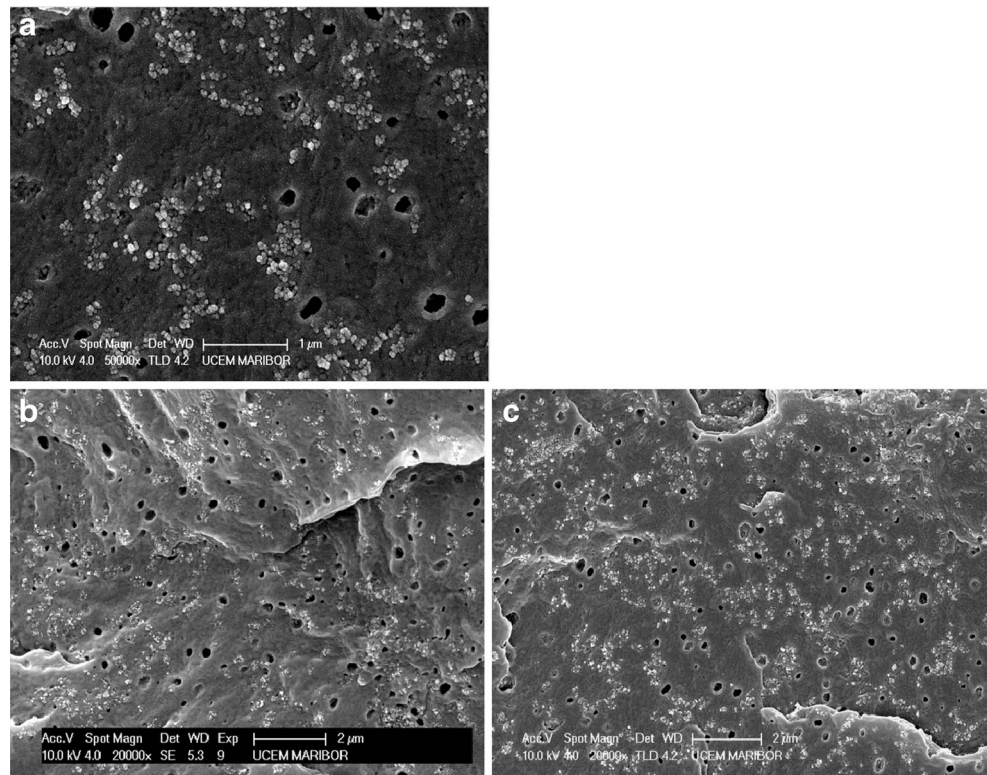

Fig. 1   Steady state torque of the iPP composites in dependance on volume content of added elastomers: a) m-EPR1 and b) m-EPR2

Fig. 2 SEM micrographs of composites with 10 phr m-EPR2: **a** hydrophilic A-200 (iPP/A-200 96/4); **b** hydrophilic A-200 (iPP/A-200 96/4) with different magnification; **c** hydrophobic A-R7200

nanosilica with both m-EPR copolymers (Fig. 2a-b). The tendency of formation of the filler-network structure in composites hydrophilic A-200 filler could be concluded by comparing SEM micrographs of these composites (Fig. 2a-b) with hydrophobic composites containing A-R7200 filler (Fig. 2c). Micrographs of latter composite reveal agglomerates of A-R7200 nanoparticles encapsulated by m-EPR besides the agglomerates dispersed in the iPP matrix as was predicted by previous research [31]. Somewhat higher τ_M values for composite with hydrophilic A-200 nanosilica than with hydrophilic S-120 microsilica also imply that the effect of filler network of nanosilicas prevails the size effect of microparticles [30]. Moreover, nano-sized particles in microsilica S-120 also exhibits the tendency of filler network formation (Fig. 3a) in comparison to the microsilica S-D17 with preferable agglomerated particles as constituents in separated and core-shell morphology (Fig. 3b). However, this contribution to τ_M values is still lower than this one of nanosilica A-200, due to just fraction of nano-sized particles in S-120 sample, and the summary result are somewhat lower τ_M values for composites with hydrophilic microsilica S-120.

Tensile test

Young's modulus

The incorporation of silica filler into polymer matrix increases Young's modulus steadily due to reinforcing effect of filler [7–9, 12]. However, the addition of both, m-EPR1 and m-EPR2

elastomers to the iPP/silica composite decreases composite stiffness almost linearly nevertheless of silica type (Figs. 4a,b) similar to the additions of SEBS and SEBS-*g*-MA elastomers [18, 19]. The similarity in Young's modulus behavior of composites with different fillers may indicate two competitive effects: the stiffening effect of the filler [7–9, 12] and the toughening effect of the elastomer [18, 19] rather than morphological or microstructural effects [23, 37] on Young's modulus.

An almost linear decrease of close E values are in accordance with the parallel model [38] where linear combination of plastic and elastomeric components were replaced with the conceivable linear combination of reinforced plastic polypropylene and toughening elastomeric components.

Final decrease of Young's modulus in this iPP/silica/m-EPR ternary composites is obviously caused by prevailing toughening effect of the m-EPR elastomer over stiffening effect of silica filler. Somewhat stronger decline in the case composites with m-EPR2 (Fig. 4b) than m-EPR1 (Fig. 4a) indicates faster decline of Young's modulus due to significantly lower molecular weight (viscosity) of m-EPR2 than m-EPR1 copolymer. Moreover, somewhat lower E values for composites with S-D17 than for other fillers indicates additional effect related with spherulite size (see discussion further).

Yield stress and strain (tensile strength and elongation at yield)

While yield stress gives additional information on filler–polymer matrix interactions in binary composites, the elastomers

Fig. 3 SEM micrograph of the iPP/S-120 96/4 with **a** 10 phr m-EPR1, **b** 10 phr m-EPR2
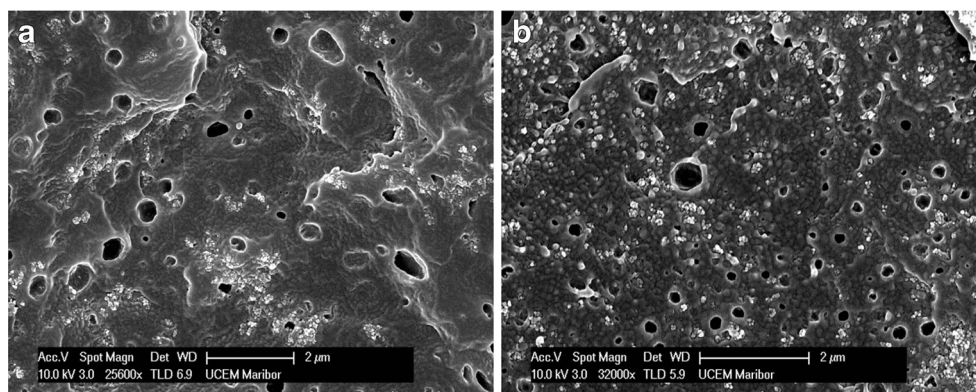
might affect yield stress as impact modifiers [2, 3]. Monotonous decreases of σ_y values with addition of both, m-EPR1 and m-EPR2 elastomers to the iPP/silica composite (Figs. 5a,b) indicates significant effect of both m-EPR elastomers on yield stress of the iPP/silica composites.

Close σ_y values and their almost linear decrease for composites with S-120, A-200 and A-R7200 (linear fitting in Figs. 5a,b) indicates that the strong toughening effect of m-EPR elastomers abolishes any difference in stiffening effect of different fillers. Somewhat lower σ_y values for composites with S-D17 that exhibit well-developed spherulites (line fitting in Figs. 5a,b) are discussed in relation to the change of intraspherulite yielding to interspherulitic boundary failure (see further discussion). This effect is more expressive in σ_y than E values (Fig. 4).

Yield strain, ε_y, of neat semicrystalline iPP depends on the strengthening of tie molecules, the intercrystalline and interspherulitic links before stretching of composite test specimen. The incorporation of silica filler into neat iPP decreases the elongation at yield ε_y due to reinforcing effect of the silica particles [25], whereas the addition of elastomers increases strain due to the toughening effect. The addition of both m-EPR elastomers to the iPP/silica composites increases the yield strain slightly; ε_y values of composites with m-EPR1 increase

almost linearly but with increased divergence (low R in Fig. 6a), whereas for composites with with m-EPR2 increase parabolically (Fig. 6b). Slightly higher ε_y values for composites with m-EPR2 than with m-EPR1 have been observed due to better stress transfer from softer m-EPR2 particles as bumpers to the iPP matrix thus causing higher elongations with regard to stiffer m-EPR1 particles. However, additional explanation could not be provided due to small changes and increased divergence of ε_y values with increased m-EPR content. It is interesting that yield behavior of these composites is very similar to the PP/wollastonite/m-EPR composites [39].

Tensile strength and elongation at break

Although the incorporation of four fillers and two elastomeric modifiers into iPP matrix has complex influence to the tensile strength at break, σ_b values of ternary iPP/SiO$_2$/m-EPR composites decrease with increased elastomer content (Fig. 7a,b) similarly to yield strength. The monotonous decrease of σ_b values with addition of both, m-EPR1 and m-EPR2 elastomers to the iPP/silica composite (Figs. 7a,b) confirms prevailing toughening effect of m-EPR elastomers over reinforcing effect of silica fillers. Almost linear decrease of σ_b values for
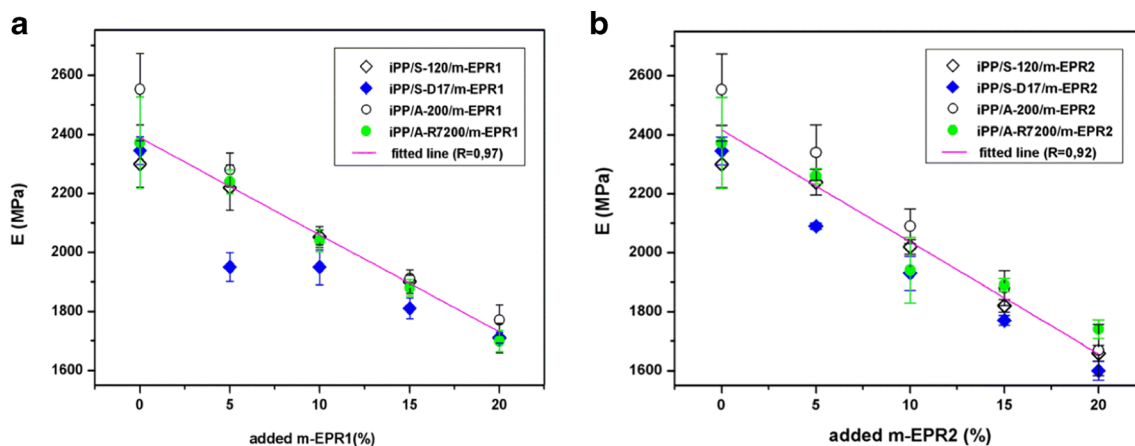

Fig. 4 Young's modulus of ternary iPP/SiO$_2$/m-EPR composites in dependence on volume content of added elastomers: **a** m-EPR1 (fitted line includes composites with S-120, A-200 and, A-R7200 fillers) and **b** m-EPR2 (fitted line includes all composites)
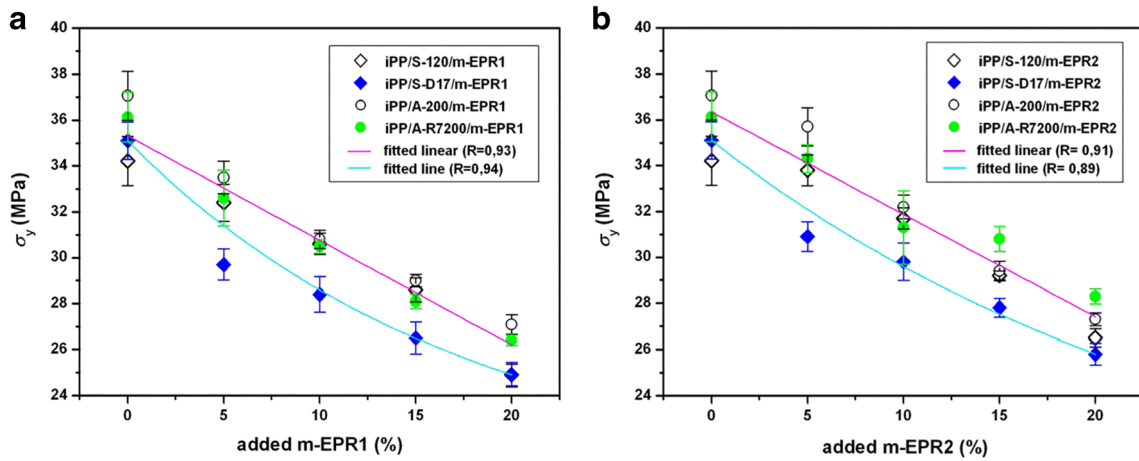
Fig. 5 Tensile strength at yield of the iPP/SiO$_2$/m-EPR composites in dependence on volume content of added elastomers: **a** m-EPR1 and **b** m-EPR2 (Upper fitted line (magenta) includes composites with S-120, A-200 and, A-R7200 fillers, while bottom fitted line (cyan) includes composites with S-D17 filler)

composites with S-120, A-200 and, A-R7200 (linear fitting in Fig. 7a) confirms similar strong toughening effect of m-EPR1 elastomer. The composites with S-D17 that revealed the largest spherulites exhibit the lowest σ_b values for composites with both m-EPR copolymers (Figs. 7 a,b) similarly to yield strength behaviour (Fig. 5).

However, the composites with m-EPR2 elastomer exhibit some divergence of σ_b values with increased elastomer content (Fig. 7b). The σ_b values of composites with m-EPR2 and S-D17 decrease even faster from the same reasons like in composites with m-EPR1 and S-D17. On the other side, σ_b values of composites with A-R7200 decrease very slowly and even increase at higher m-EPR2 amounts unexpectedly (Fig. 7b). It is interesting that A-R7200 nanosilica cause the growth of small irregular spherulites like S-120 and A-200, while the interfacial free energy of iPP/A-R7200 is minimal in comparison to pairs (A-R7200 (16.15 mJ/m^2) < S-D17 (16.39 mJm^{-2}) < S-120 (33.82 mJm^{-2}) < A-200 (34.31 mJm^{-2}) [31]. Most likely treated A-R7200 nanoparticles, compatible with

iPP and selectively dispersed in the iPP matrix (fine dispersion) may contribute to such behavior of σ_b values. Intermediary σ_b values of composites with hydrophilic S-120 and A-200 fillers are reasonable in respect to other two composites (Fig. 7b).

The elongation at break, ε_b, usually behaves inversely to the tensile strength at break. Really, the ε_b values increases slowly with increased m-EPR1 and m-EPR2 content (Figs. 8 a,b). They are significantly higher for composites with S-D17 than for composites with other silica fillers (especially at 20 phr of added m-EPR). The σ_b values were compared to the average spherulite diameter calculated by Eq. (1) from measured maximal and minimal diameters of each spherulite in Figs. 8a,b.

The highest ε_b values exhibit the composites with nonpolar S-D17 microsilica and the largest spherulites (Fig. 8a,b). Extremely high ε_b value of the iPP/S-D17/m-EPR1 composite at 20 phr of added m-EPR1 (please notice the different ordinate labels in Fig. 8a, b) indicates additional influencing factor
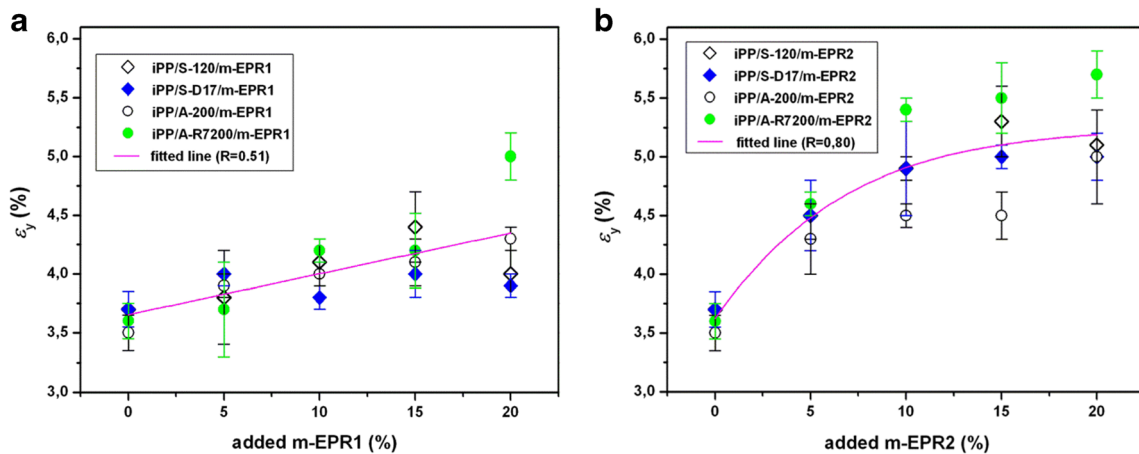

Fig. 6 Elongation at yield of the iPP/SiO$_2$/m-EPR composites in dependence on volume content of added elastomers: **a** m-EPR1 and **b** m-EPR2. Fitted line includes all composites in both figures
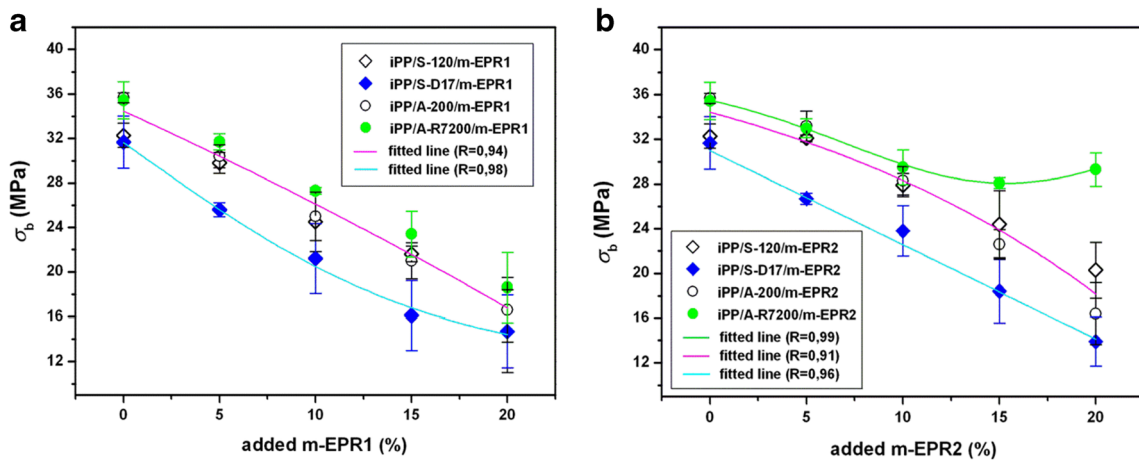
Fig. 7 Tensile strength at break of the iPP/SiO$_2$/m-EPR composites in dependence on volume content of added elastomers: **a** m-EPR1 (upper fitted line (magenta) includes composites with S-120, A-200 and, A-R7200 fillers, while bottom fitted line (cyan) includes composite with S-D17 filler) and **b** m-EPR2 (upper fitted line (green) includes composites with A-R7200); intermediary fitted line (magenta) includes composites with S-120, A-200; bottom fitted line (cyan) includes composite with S-D17 filler)

besides the spherulite size. Actually, m-EPR1 copolymer with significantly higher molecular weight than m-EPR2

copolymer (more comparable to the molecular weight of the iPP) contributing thus to extremely high ε_b value additionally.

Fig. 8 Elongation at break of the iPP/SiO$_2$/m-EPR composites in dependence on volume content of added elastomer: **a** m-EPR1 and **b** m-EPR2. (Upper fitted line (cyan) includes composites with with S-D17 filler, while bottom fitted line (magenta) includes composite with S-120, A-200 and, A-R7200 fillers)
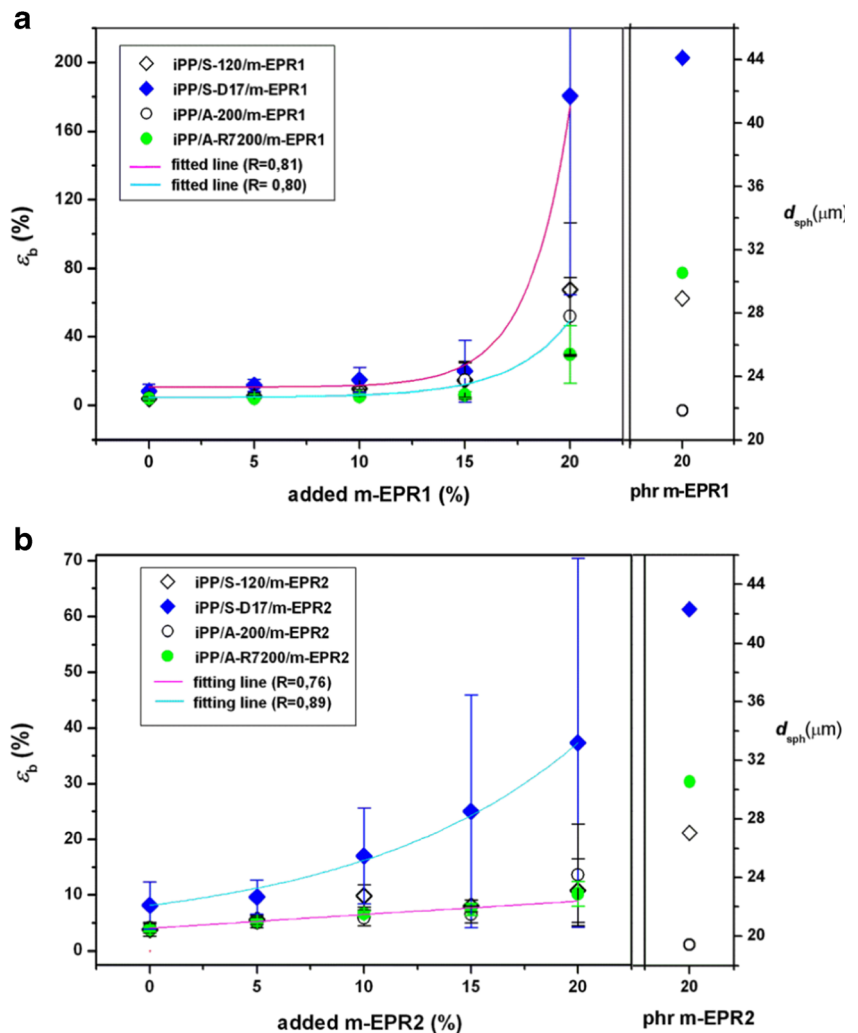
However, ε_b values of composites with S-120, A-200 and A-R7200 are very similar as well as their morphology with irregular spherulites or grains are very similar. Relatively higher difference in measured spherulite diameters is in some extent is the result of different anisotropic degrees of irregular spherulites and grains. Composites with A-R7200 nanoparticles exhibit the lowest ε_b values because elongation at break behaves inversely to the tensile strength at break (explained at corresponding before-mentioned σ_b values, respectively). On the other side, composites with hydrophilic S-120 and A-200 fillers exibit low ductility.

Impact properties

The incorporation of the silica filler usually reinforces the iPP matrix improving stiffness and tensile strength but, at the same time, reduces the toughness and deteriorates the impact strength [12]. Thereby, m-EPR elastomers were added to the binary iPP/SiO$_2$ composites in order to increase the toughness. While the notched impact strength, a_K, of the iPP/silica composites really decreases with increased silica content [12], a_K values of the iPP/SiO$_2$/m-EPR composites exponentially increases by adding of m-EPR elastomer (Fig. 9). This fact indicates a significant overcome of the elastomeric toughening effect in relation to the filler's stiffening effect. The a_K values in both iPP/SiO$_2$/m-EPR composite systems are very close, similarly to co-measurable values observed in iPP/SiO$_2$/SBC (styrenic block copolymers) composites [14, 18, 19]. Multifold increase of impact strengths for all composites with m-EPR and SBC copolymers may indicate a result of synergistic effect of introduced SiO$_2$ fillers and elastomers rather than simply compensation of reduced toughness by stiffening effect of filler by overcoming toughening effect of elastomer. Almost linear increase of the a_K values of the iPP/SiO$_2$/SBC composites [18, 19] could be explained by sum of compatibilization (due to a core-shell morphologies) and toughening effect of elastomers (in accord to addition rule) at lower and higher SBC content, respectively. Accordingly, exponential increase of the a_K values for iPP/SiO$_2$/m-EPR composites could be the result of negligible compatibilization effect at lower m-EPR content due to prevailing separated morphology in these systems [31].

Moreover, somewhat higher a_K values of composites with m-EPR1(more than five-fold increase) than m-EPR2 (about four-fold increase) have been observed due to higher molecular weight of m-EPR1 than m-EPR2 copolymer. This effect of molecular weight is similar to an effective compatibilizer which must have a high enough molecular weight (chain length comparable to this one of the iPP); larger iPP or olefins segments can penetrate more easily into corresponding iPP matrix and provide strong entanglements improving thus the notched impact strength and elongation. On the other side, shorter molecules of m-EPR2 copolymer act as plasticizer rather than impact modifier. Relatively high a_K values of composites with hydrophilic SiO$_2$ fillers could be related to formation tendency of filler network in ternary PP/EPDM/SiO$_2$ system facilitated by higher elastomer content (20 phr) in accordance to the literature findings [34, 35].

Effect of interfacial properties, structure and morphology on mechanical properties

Basically, the mechanical behavior of ternary iPP/SiO$_2$/m-EPR composites could be considered as the conceivable linear combination of competitive effects of reinforced plastic polypropylene and toughening elastomeric components. However, prominent mechanical characteristics of some samples indicate superimposing effects of adhesion, structure and morphology to this combination of basic reinforcing and toughening effects. Interfacial properties may affect mechanical properties directly by the interaction between the polymer matrix and the dispersed filler and elastomer particles and indirectly by affecting the agglomeration, filler network formation, ultimate morphology of composites as well as the spherulitic morphology. In previous paper it was established that iPP/SiO$_2$/m-EPR composites exhibit preferable morphology with SiO$_2$ and m-EPR particles separately dispersed in the iPP matrix, while other complex morphologies are present in minor extent [31]. Accordingly, direct effect of adhesion on mechanical properties should be examined by consideration of the iPP-elastomer and iPP-filler interactions. While the difference between interfacial free energy of the iPP—m-EPR1 and iPP—m-EPR2 are negligible, interfacial free energy between iPP and hydrophilic fillers are twofold higher than between iPP and hydrophobic fillers [31]. These differences in the interfacial interaction between iPP-polar and iPP-nonpolar fillers have resulted in ultimate morphology. The presence of micron-sized S-D17 particles at fractured and microtomed surfaces confirmed such interfacial properties of the iPP/S-D17/m-EPR composites [31]. Contrary, the absence of micron-sized S-120 particles at fractured samples in presented SEM micrograph (Fig. 10) confirmed low compatibility of this filler with iPP matrix. Great number of holes (several microns in size) indicate the tendency of micron-sized S-120 particles (pulled-out) to locate at interspherulitic boundaries and their heterogenous dispersion along homogenenous dispersion of smaller particles. Accordingly, minimal interfacial tension at iPP—S-D17 interface indicates the strongest compatibility iPP with S-D17 filler that should lead to improved tensile strength of these composites. Paradoxal result, the lowest tensile strengths parameters (σ_y and σ_b), lower E values and, the highest elongations of the composites with nonpolar S-D17 silica filler indicate that the effect of interfacial interactivity was prevailed by other effect(s).

Moreover, interfacial properties favored formation of separated morphologies [28] and filler network as well as
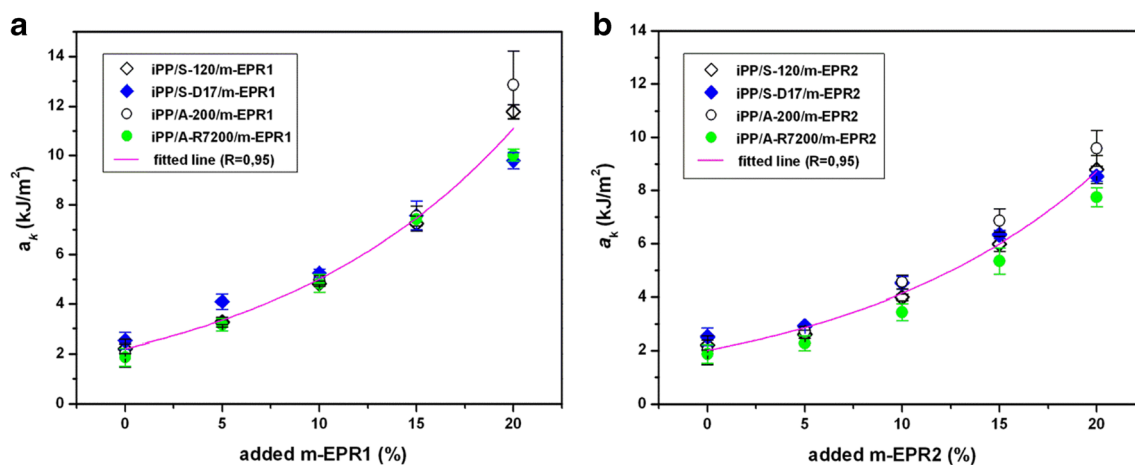
Fig. 9 Notched impact strength of the iPP/SiO$_2$/m-EPR composites in dependence on volume content of added elastomers: **a** m-EPR1 and **b** m-EPR2. Fitted line includes all composites in both figures

consequent mechanical properties. Higher agglomeration degree of the hydrophilic than the hydrophobic silicas in binary iPP/SiO$_2$ composites could increase torque values only at higher silica contents (>4 vol%) [6, 12, 40]. However, in present ternary composites with constant iPP/SiO$_2$ ratio 96/4 the formation tendency of the filler network in composites with hydrophilic silica fillers (Figs 2,3) might affect rheological and mechanical properties. In according to literature findings [34, 35] filler-filler network may improve torque values and toughness. Somewhat higher a_K values of composites with hydrophilic SiO$_2$ fillers (Fig. 9) could be exactly related with formation tendency of filler network like in ternary PP/EPDM/SiO$_2$ system facilitated by higher elastomer content (20 phr) [34, 35]. Moreover, different nucleation ability of silica particles caused by character of the iPP-filler interface could be reflected on spherulite growth (see further). Although the interfacial properties favored formation of separated morphologies [31] filler network and consequent mechanical
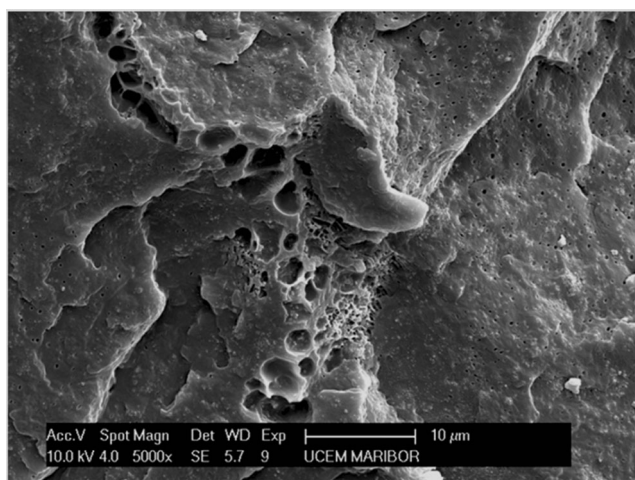

Fig. 10 SEM micrograph of the iPP/S-120/m-EPR2 composites exhibits the absence of bigger S-120 microparticles at fractured samples

properties, as well as spherulitic morphology, mechanical behavior is affected by other factors. Separated morphology also implies that m-EPR elasomers preferable act as impact modifiers, whereas their compatibilization effect could be neglected. The effect of the difference in segmental microstructure of m-EPR's [31] on mechanical properties is rather questionable. However, there are two significant differences between these two elastomers that may affect mechanical properties. First, m-EPR1 has almost twice higher molecular weight than m-EPR2 and MFI value commensurable with the iPP (Table 1). It is well known fact that the polymer with longer macromolecules exhibits higher toughness. At the same time m-EPR2 copolymer has more than twice lower molecular weight than iPP (more than twice shorter macromolecules) and may act as the plasticizer rather than the impact modifier. Secondly, m-EPR2 copolymer is more compatible or partially miscible with iPP matrix as was supposed by the interfacial properties [31]. TEM micrograph in Vistamaxx Overview [27] indicated the compatibility of both m-EPRs with i-PP; the blending results in the lamellar (co)crystallization across phase boundary or in the diffuse inter-phase. Higher elastomer content (20 phr) also facilitated, beside formation of filler network, spherulite growth by prolonged crystallization due to migration of iPP chains from the remained melt islands of the m-EPR elastomer toward the iPP matrix during solidification of molten composite. As was mentioned above, it is paradoxical that the composites with nonpolar S-D17 silica filler compatible with iPP matrix exhibit the lowest tensile strength properties (σ_y and σ_b), lower E values and, the highest elongations. This fact indicates that some structural or morphological characteristics affect mechanical properties stronger than interfacial properties. It was proved that the mechanical properties of semicrystalline polymers strongly depend on the crystallinity [41, 42]. Although the effect of crystallinity and spherulite size on fracture depends on the same structural characteristics (the lamellar build-up and the tie-chains density) the effect of spherulite

Fig. 11 Tensile strength as a function of spherulite size according to refs. [45, 48, 49]
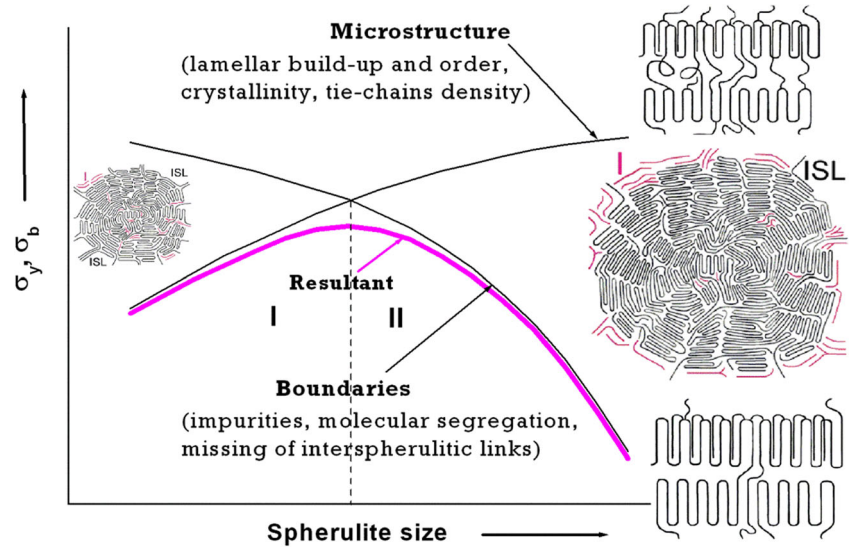
size on mechanical properties is still ambiguous [16, 23]. Although earlier papers confirmed the decrease of yield strength by increasing spherulite size [43], some research papers established that an increase in brittleness may appear at nucleated small spherulites as well as at increased spherulite size at constant crystallinity [44, 45]. Taking into account this fact Way et al. have reconciled these two contrarieties by two contributions; the microstructure effect, which results in greater crystallinity and strength; and the spherulite boundary effect, whereby the boundaries become progressively weaker [45]. Karger-Kocsis et al. [46, 47] specified the influencing factors which resulted in maximum related to the change from intraspherulite yield (stage I) to interspherulitic boundary failure (stage II). First process is controlled by microstructural (intraspherulitic) factors important for stress transfer (crystallinity, lamellar build-up and order, tie-chains density) (increasing line in Fig. 11). Decohesion process along the spherulite boundaries promoted failure by weakening interspherulitic boundary due to present impurities and segregated low molecules, as well as the lack of interspherulitic tie macromolecules (decreasing line in Fig. 11) [46, 47]. Resultant curve exhibits maximum at optimal combination of all factors – cross-section of two two curves. Because present iPP/S-D17/m-EPR composites with enlarged spherulites exhibit the lowest tensile strength properties (σ_y and σ_b), lower E values and the highest elongations they could be located at rigth side in comparison to maximum and to other composites which could be located at left side (Fig. 11). Because of lower strength values of this composite in comparison to other composites due to weaker interspherulitic boundaries they would be located at lower level on resultant curve.

(ISL = interspherulitic links, I = impurities and segregated molecules).

Analogously to tensile strength behavior, toughness or ductiliy are not depended on spherulite size. Comparable impact

strength values for composites with S-D17 (large spherulites) and those ones with A-R7200 (small irregular spherulites) even
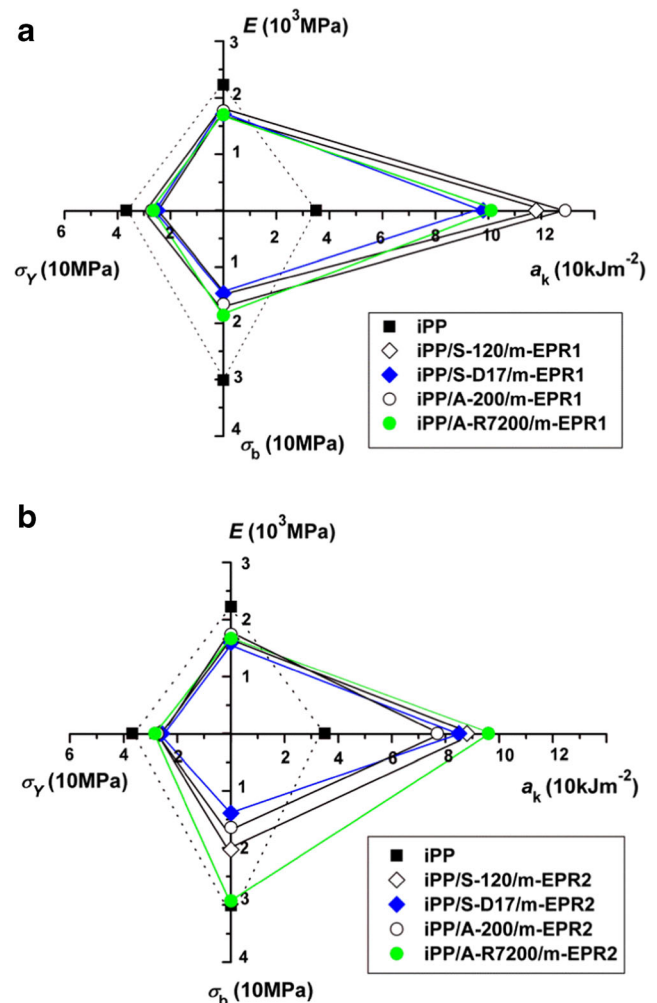

Fig. 12 Optimization diagrams of mechanical properties of iPP/SiO$_2$/m-EPR1 and iPP/SiO$_2$/m-EPR2 with 20 phr of added elastomers

at 20 phr m-EPR (Fig. 9) confirm this conclusion. Actually, the fracture toughness slightly decreases with increasing spherulite size (at a constant crystallinity), but reduced toughness might also appear in material with nucleated, very fine spherulites due to facilitating crack growth [44]. Friedrich has been reconciled these two contrarieties by two competetive deformation mechanisms the process of which is as the functions of spherulite size: plastic deformation (reorganization and destruction of the lamellae by sliding and defolding of lamellar blocks and voiding of amorphous regions) and interspherulitic fracture (boundary effects, forming crazes by coalescence of cavities) [48, 49]. Resultant deformation or crazing curve exhibits the maximum at cross section of these two competetive processes analogously to the tensile strength features [48, 49]. Higher deformation values of composites with S-D17 implies their location at higher level on crazing curve in comparison to other with reduced ductility due to facilitating crack growth by nucleated very fine spherulites [44].

Optimization diagrams of mechanical properties

Mechanical properties are one of the most respected criteria for choosing right materials for some end-use purpose. Schematic diagrams show the change in some important materials properties by introducing one or two components in polymer matrix. The optimization diagrams of such design materials were used for comparing their mechanical parameters with the pure isotactic polypropylene. Optimization diagrams in Figs. 12a,b exhibit somewhat lower tensile strengths and Young's modulus but also three times larger impact strength of the iPP/silica/m-EPR composites than plain iPP, simultaneously. The composites with longer elastomeric m-EPR1 macromolecule (Fig. 12a), especially in combination with untreated silica fillers (S-120 and A-200 that nucleate small irregular spherulites), exhibit the highest toughness (about six-fold increase) and could be offered as material with designed toughness. Very close Young's modulus values E for both iPP/SiO$_2$/m-EPR systems (Figs 4 a,b) are still higher than for the iPP/SiO$_2$/SBC composites at 20 phr elastomer [18, 19]. Moreover, the composite with m-EPR2 in combination with methacrylsilanized A-R7200 nanosilica exhibit the highest ultimate tensile strength σ_b significantly higher than those ones of the the iPP/SiO$_2$/SBC composites [18, 19] and even co-measurable with this one of plain iPP due to morphology with small irregular spherulites (see Figs. 7b and 12b). The values of elongation at break were not included in these diagrams because of their large divergence/scattering at 20 phr m-EPRs. However, composite with nonpolar S-D17 microsilica, especially in combination with m-EPR1 elastomer, exhibit extremely high ductility (Fig. 8). Accordingly, metallocenic m-EPR elastomers are really good and prominent modifiers in combination with particular silica fillers for desired mechanical properties.

Conclusions

The effects of four silica fillers differing in size (nano- vs. micro-) and in their surface properties (hydrophilic vs. hydrophobic, e.g. polar vs. non-polar) with constant 96/4 volume ratio and varied contents of two m-EPR elastomers (2,5–20 phr) differing in molecular weights (e.g. viscosity) as well as interfacial properties and morphologies on rheological and mechanical properties of the iPP/SiO$_2$/m-EPR composites were discussed. Rheological properties of molten iPP/SiO$_2$/m-EPR composites were affected by the viscosity of applied elastomers, the interfacial properties determined by filler surface properties, the probable formation of the hydrophilic filler-network structure (nanosized prevailed over microsized particles forming network) and the dispersion of particles and agglomerates size as well. The iPP/SiO$_2$/m-EPR composites exhibit preferable morphology with SiO$_2$ and m-EPR particles separately dispersed in the iPP matrix, while other complex morphologies are present in minor extent [31].

Young's modulus were influenced mainly by the linear combination of reinforced plastic polypropylene and toughening elastomeric components. Tensile properties were additionally affected by intraspherulitical and interspherulitical characteristics of the iPP matrix as well as by the length of m-EPR macromolecule. The fact that the composites with nonpolar S-D17 silica filler are the most compatible with nonpolar iPP matrix and exhibited the lowest tensile strength properties (σ_y and σ_b) and lower E values indicated negligible effect of fillers on mechanical properties. However, the characteristics of the silica filler surface are defined by the nucleation (dis)ability of (non)polar fillers that lead to difference in spherulitic morphology [31]. As the result of competetive effects of intraspherulitic and spherulite boundaries characteristics, composites with mentioned nonpolar S-D17 silica filler (with the largest spherulites) exhibited lower tensile strength and Young modulus values in comparison to composites with other silica fillers that nucleated smaller irregular spherulites.

Similarly, composites with nonpolar S-D17 silica filler exhibited higher ductility than other composites due to higher deformation possibility as a result of two competetive deformation mechanisms: the homogeneous, plastic deformation and the interspherulitic fracture. Moreover, almost twice longer m-EPR1 than m-EPR2 macromolecule exhibited increased ductility and toughness of composites. Hydrophilic SiO$_2$ fillers increased the toughness of the composites additionally, due to formation tendency of the filler network facilitated by higher elastomer content (20 phr). On the other hand, m-EPR2 copolymer with lower molecular weight than iPP and more compatible and miscible with iPP matrix might participate in the building diffuse and the lamellar inter-phase. Prevailing separated morphology of ternary iPP/SiO2/m-EPR composites [31] implies that m-EPR elasomers preferable act

as impact modifiers (Fig. 11), whereas their compatibilization effect could be neglected.

Obviously, design of the iPP/SiO$_2$/m-EPR composites could be possible due to different characteristics of introduced SiO$_2$ and m-EPR components, effects and interactions; stiffening effect of the filler, toughening effect of the elastomer, length of the m-EPR macromolecule, nucleation ability of filler and separated morphology determined by interfacial properties, intra- and interspherulitical structure and crazing mechanism some of them in synergistic way.

References

1. Karian HG (2003) Handbook of polypropylene and polypropylene composites. Marcel Dekker, New York

2. Wypych G (2000) Handbook of fillers. ChemTec Publishing, Toronto

3. Rothon RN (2006) Particulate-Filled Polymer Composites. Rapra, Shawbury

4. Karger-Kocsis J, Fakirov S (2010) In: Karger-Kocsis J, Fakirov S (eds) Nano- and micromechanics of polymer blends and composites. Munich, Carl Hanser Verlag

5. Rothon RN (2010) In: Xanthos M (ed) Functional Fillers for Plastics. Weinheim, Wiley-VCH Verlag

6. Pustak A, Pucić I, Denac M, Švab I, Pohleven J, Musil V, Šmit I (2013) J Appl Polym Sci 5:3099–3106

7. Bikiaris DN, Papageorgiou GZ, Pavlidou E, Vouroutzis N, Palatzoglou P, Karayannidis GP (2006) J Appl Polym Sci 100: 2684–2696

8. Rong MZ, Zhang MQ, Zheng YX, Zeng HM, Walter R, Friedrich K (2001) Polymer 42:167–183

9. CL W, Zhang MQ, Rong MZ, Friedrich K (2002) Compos Sci Technol 62:1327–1340

10. Zhou TH, Ruan WH, Mai YL, Rong MZ, Zhang MQ (2008) Compos Sci Technol 68:2858–2863

11. Vassiliou A, Bikiaris DN, Pavlidou E (2007) Macromol React Eng 1:488–501

12. Pustak A, Leskovac M, Denac M, Švab I, Pohleven J, Makarovič M, Musil V, Šmit I (2014) J Reinf Plast Compos 33:851–861

13. Dabrowska I, Fambri L ,Pegoretti A,Slouf M, Vackova T, Kolarik J (2015) Express Polym Lett 9: 277–290

14. Wang W-Z, Liu TJ (2008) Appl Polym Sci 109:1654–1660

15. Mae H, Omiya M, Kishimoto KJ (2008) Appl Polym Sci 110: 1145–1157

16. El-Midany AA, Ibrahim SS (2011) Physicochem Probl Miner Process 46:295–305

17. Panaitescu DM, Vulunga Z, Notingher PV, Nicolae C (2013) Polym Eng Sci 53:2081–2092

18. Pustak A, Denac M, Leskovac M, Švab I, Musil V, Šmit I (2015a) J Appl Polym Sci 132:41486–41498

19. Pustak A, Denac M, Leskovac M, Švab I, Musil V, Šmit I (2015b) Polym –Plast Technol 54: 647–660

20. Bikiaris DN, Vassiliou A, Pavlidou E, Karayannidis GP (2005) Eur Polym J 41:1965–1978

21. Buaziz A, Jaziri M, Dalmas F, Massardier V (2014) Polym Eng Sci 54:2187–2196

22. Chen JH, Rong MZ, Ruan WH, Zhang MQ (2009) Compos Sci Technol 69:252–259

23. Uotila R, Hippi U, Paavola S, Seppala J (2005) Polymer 46: 7923–7930

24. Martin G, Barres C, Sonntag P, Garois N, Cassagnau P (2009) Mater Chem Phys 113:889–898

25. Bazgir S, Katbab AA, Nazockdast HJ (2004) Appl Polym Sci 92: 2000–2007

26. Mokhothu TH, Luyt AS, Messori M (2014) Express Polym Lett 8: 809–822

27. VISTAMAXX™ Specialty Elastomers (2004) General technical overview. Exxon Mobil, Belgium

28. Cheng C, Racine G, Srinivas S, Datta S (2004) Novel Propylene-Based Specialty Elastomers: Structure and Properties. Proceedings of ANTEC, 62nd Annual technical conference, Chicago: 4220–422

29. Hemmati HN, Nazokdast H, Panahi HSJ (2001) J Appl Polym Sci 82:1129–1137

30. Das S, Murthy VSR, Murty GSJ (1999) Mater Sci 34:1347–1352

31. Pustak A, Denac M, Leskovac M, Švab I, Musil V, Šmit I (2016) J Polym Res 23:1–12

32. Payne AR, Whittaker RE (1971) Rubber Chem Technol 44: 440–478

33. Freund B, Niedermeier W, Kautsch Gummi Kunstst (1998) 51: 444–449

34. Yang H, Zhang Q, Guo M, Wang C, Du R, Fu Q (2006) Polymer 47:2106–2211

35. Yang H, Zhang X, Qu C, Li B, Zhang L, Zhang Q, Fu Q (2007) Polymer 48:860–869

36. Yang H , Li B , Wang K, Sun T, Wang X, Zhang Q, Fu Q, Dong X, Han CC (2008) Euro Polymer J 44: 113–123

37. Hornsby PR, Premphet K (1998) J Appl Polym Sci 70:587–597

38. Gedde UW (1995) Polymer Physics. Chapman and Hall, London

39. Švab I, Musil V, Pustak A, Šmit I (2009) Polym Compos 30:1091–1097

40. Manias E, Polizos G, Nakajima H (2007) Fundamentals of polymer nanocomposite technology. In: Morgan AB, Wilkie CA (eds) Flame retardant polymer nanocomposites. Wiley-Interscience, Hoboken, pp. 31–66

41. Mills NJ (1993) Plastics: Microstructure and Engineering Applications. Elsevier, London, pp. 170–198

42. Ghosal AK (2008) Crystallization of Isotactic Poly(Propylene) with Enachanted MeltStrenght, PhD thesis. http://diginole.lib.fsu.edu/islandora/object/fsu%3A182478 (acessed May 2016)

43. Starkweather HW, Brooks RE (1959) J Appl Poylm Sci 1:236–239

44. Ouederni M, Phillips PJ (1995) J Polym Sci B Polym Phys 33: 1313–1322

45. Way JL, Atkinson JR, Nutting J (1974) J Mater Sci 9:293–299

46. Karger-Kocsis J (1995) Microstructural aspects of fracture in polypropylene and in its filled, chopped fiber and fiber mat reinforced composites. In:. Karger-Kocsis J (ed) Polypropylene: Structure blends and composites Vol. 3 Composites Springer, Dordrecht, Chapter 4:142–201

47. Bárány T, Czigány T, Karger-Kocsis J (2010) Prog Polym Sci 35: 1257–1287

48. Friedrich K (1979) *Kunststoffe* 69:796–801

49. Friedrich K (1983) Crazes and shear bands in semi-crystalline thermoplastics. In: Kausch HH (ed) Adv Polym Sci: Crazing in Polymers, Springer, Berlin, Vol 52/53: 225–274